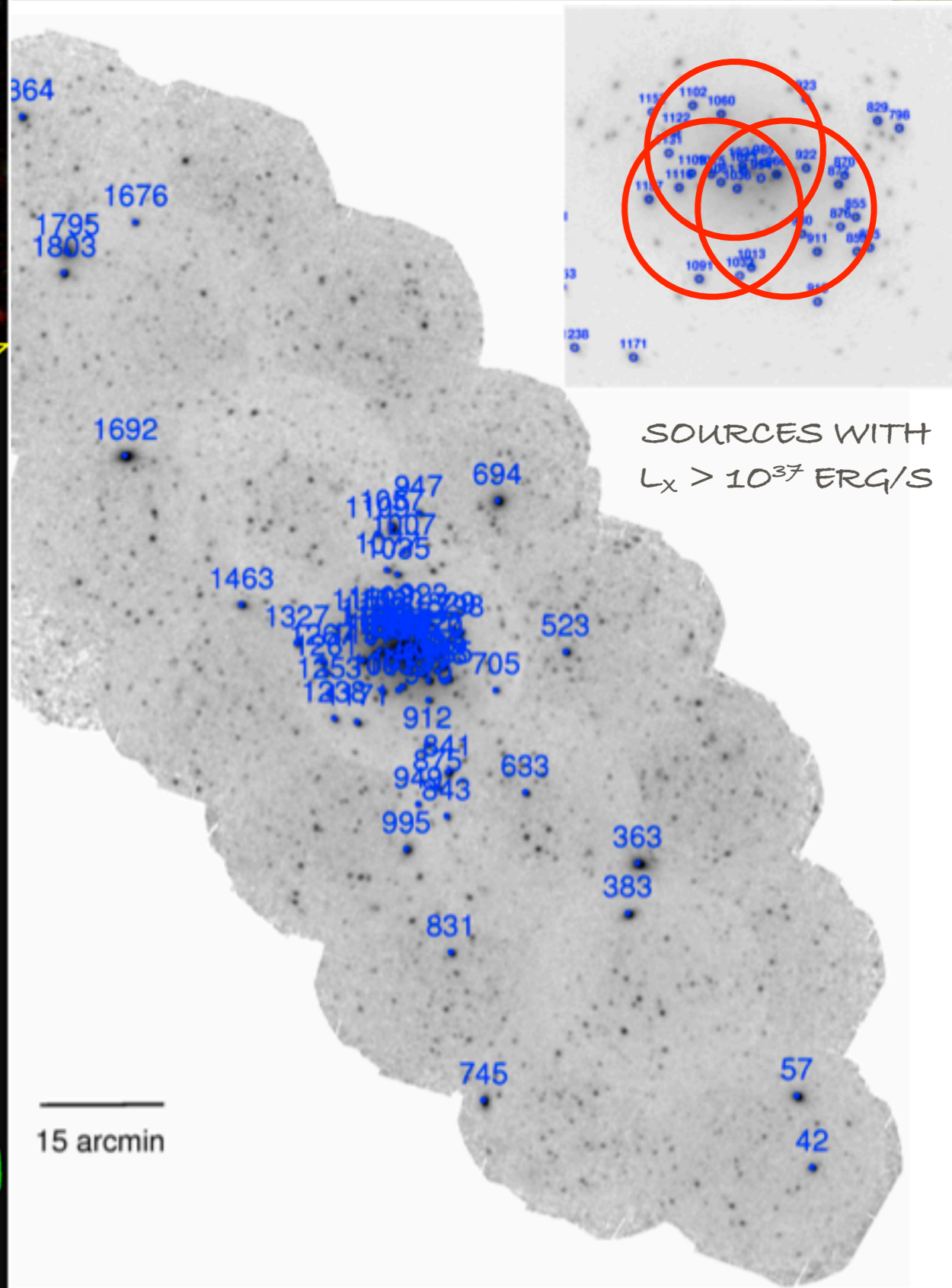
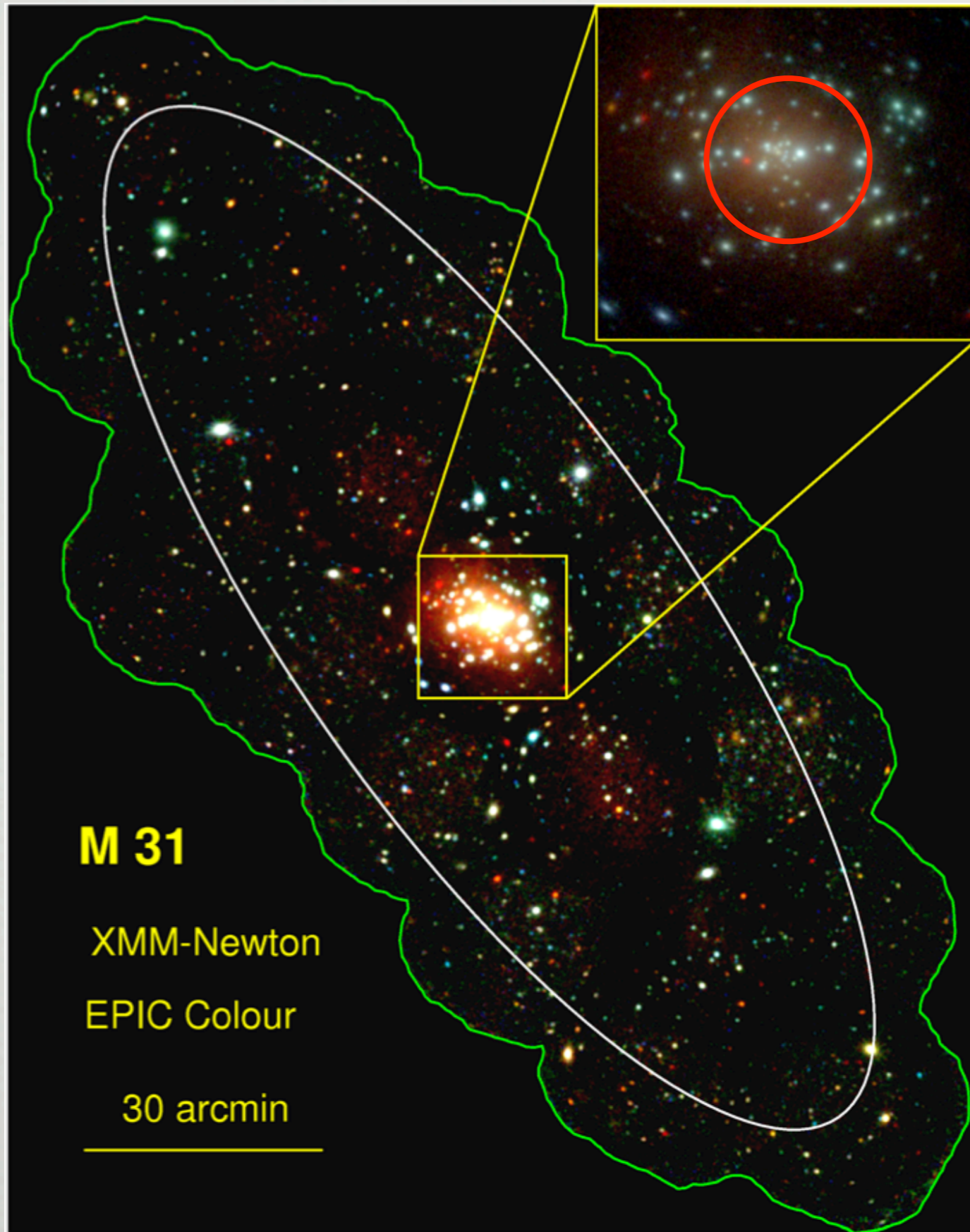
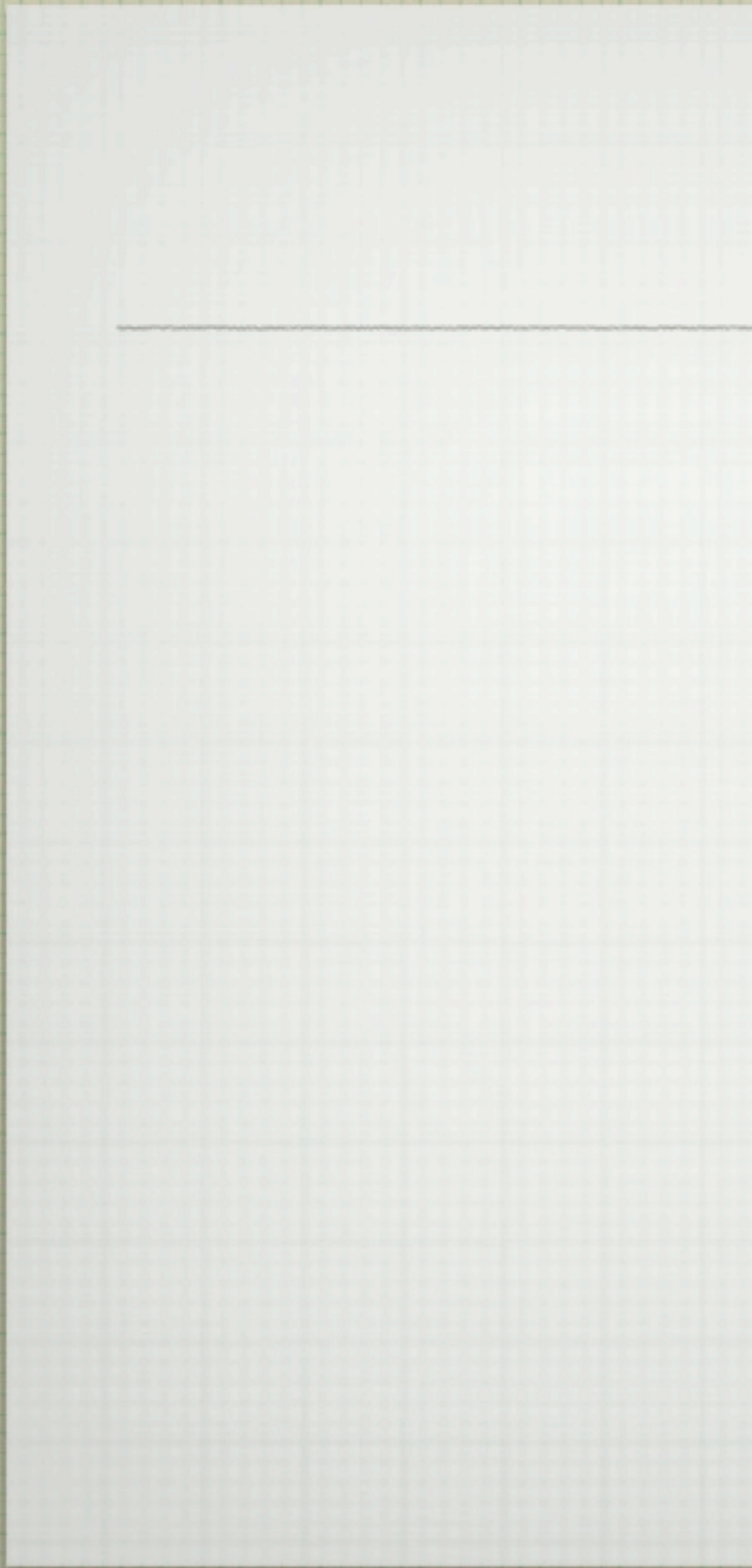


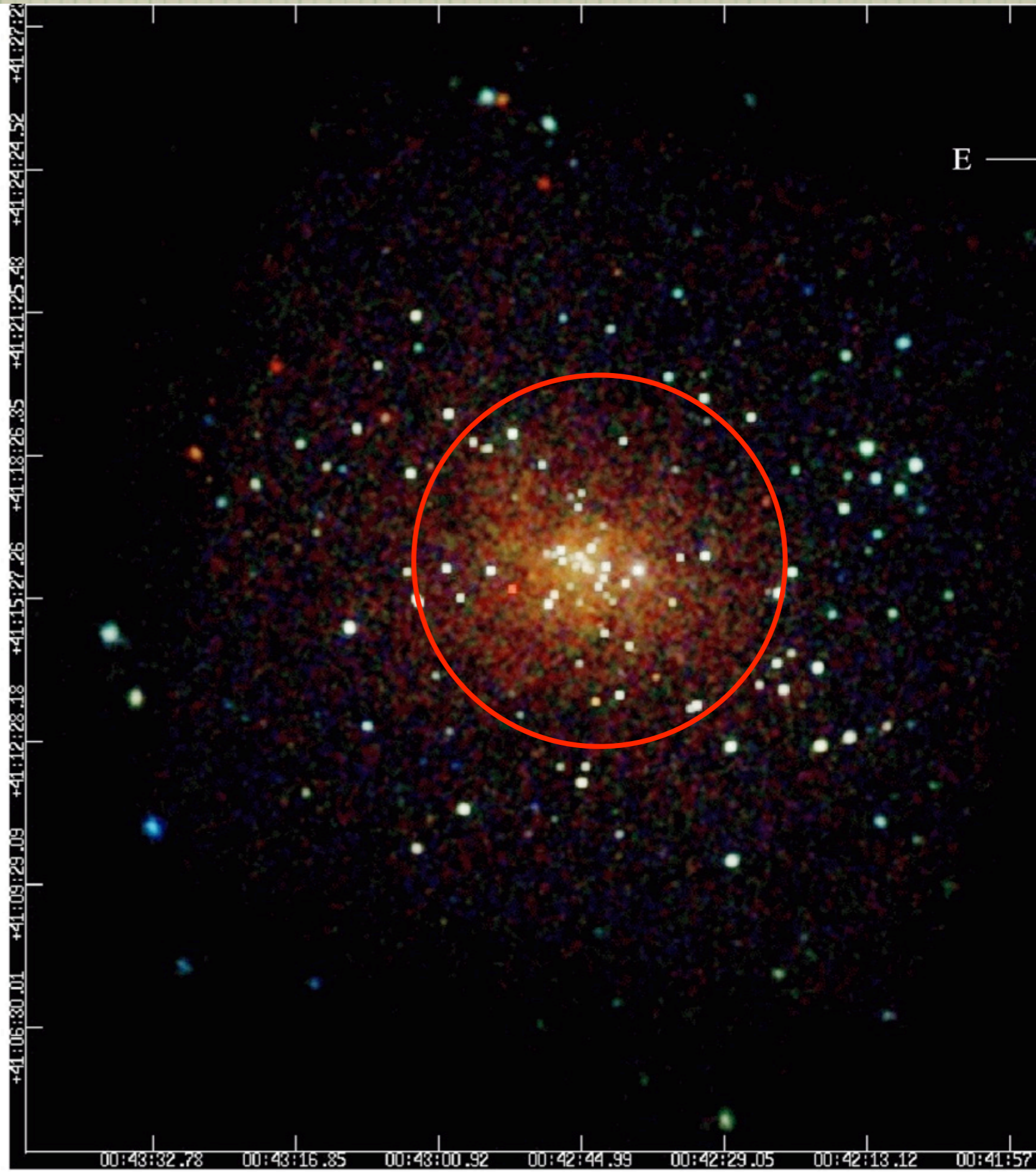
GRATING SPECTROSCOPY OF THE M31 BULGE

HERMAN L MARSHALL

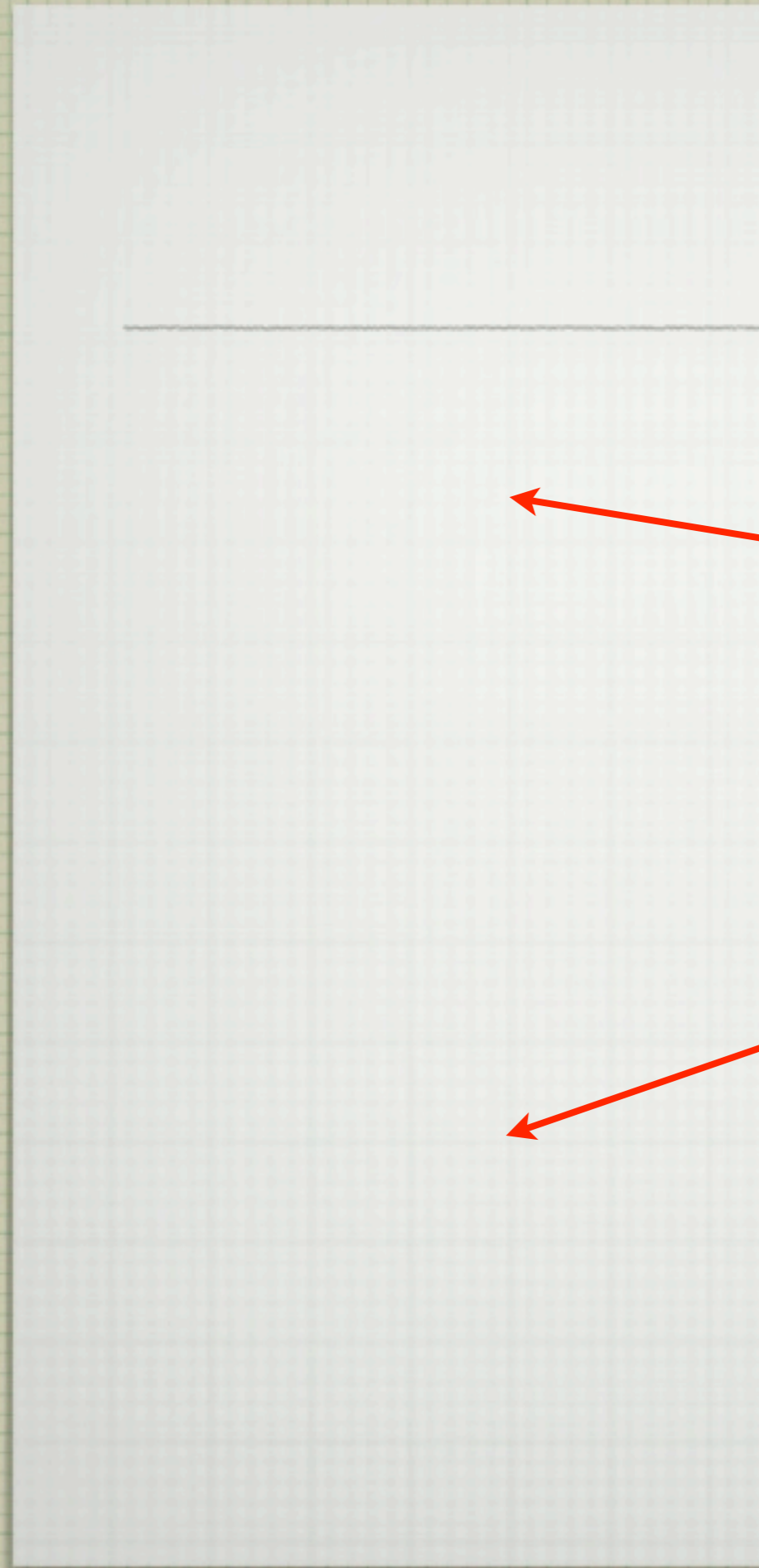




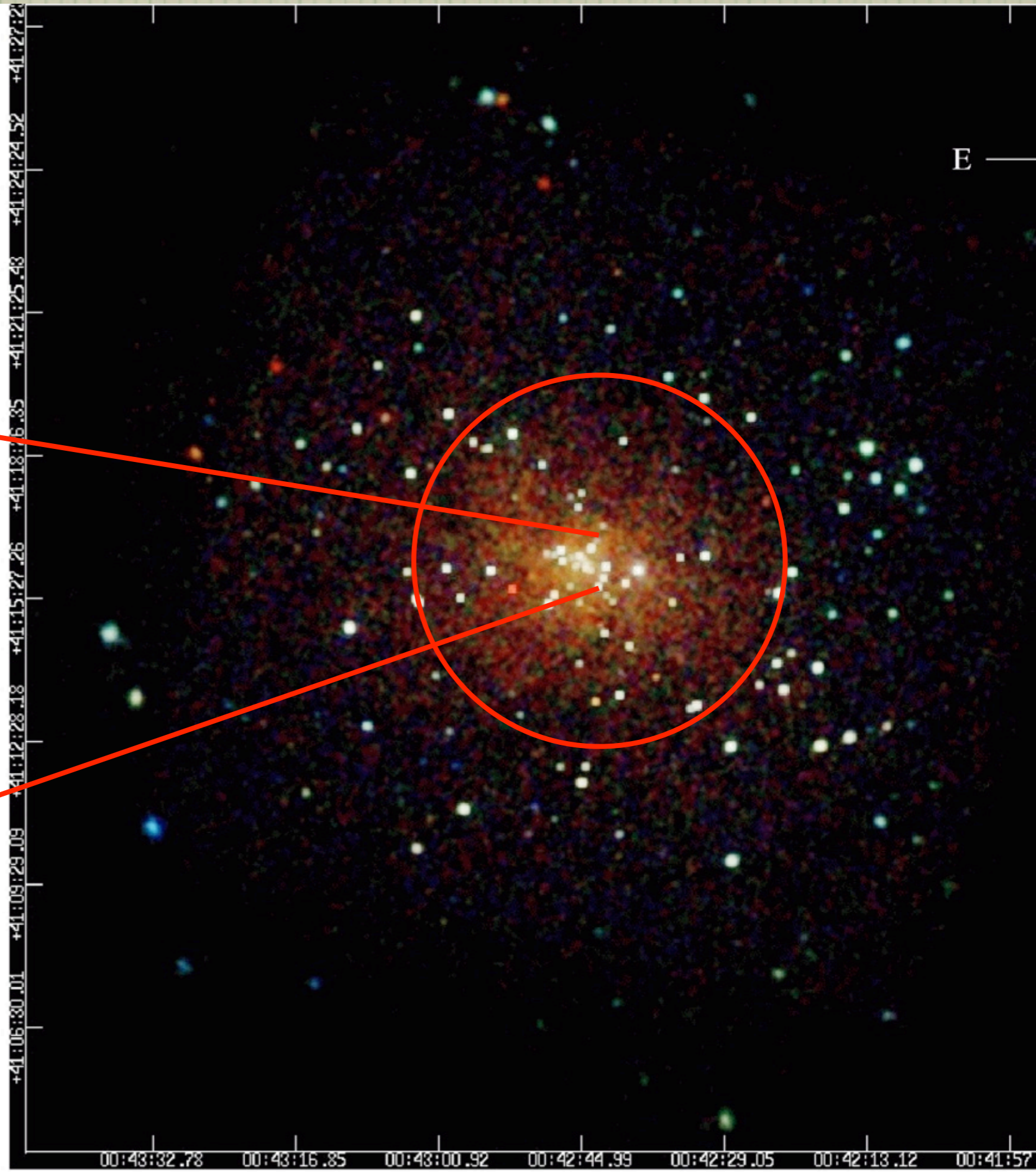
Dec. (J2000)



R.A. (J2000)



Dec. (J2000)



R.A. (J2000)

00:43:32.78
+41:27:22

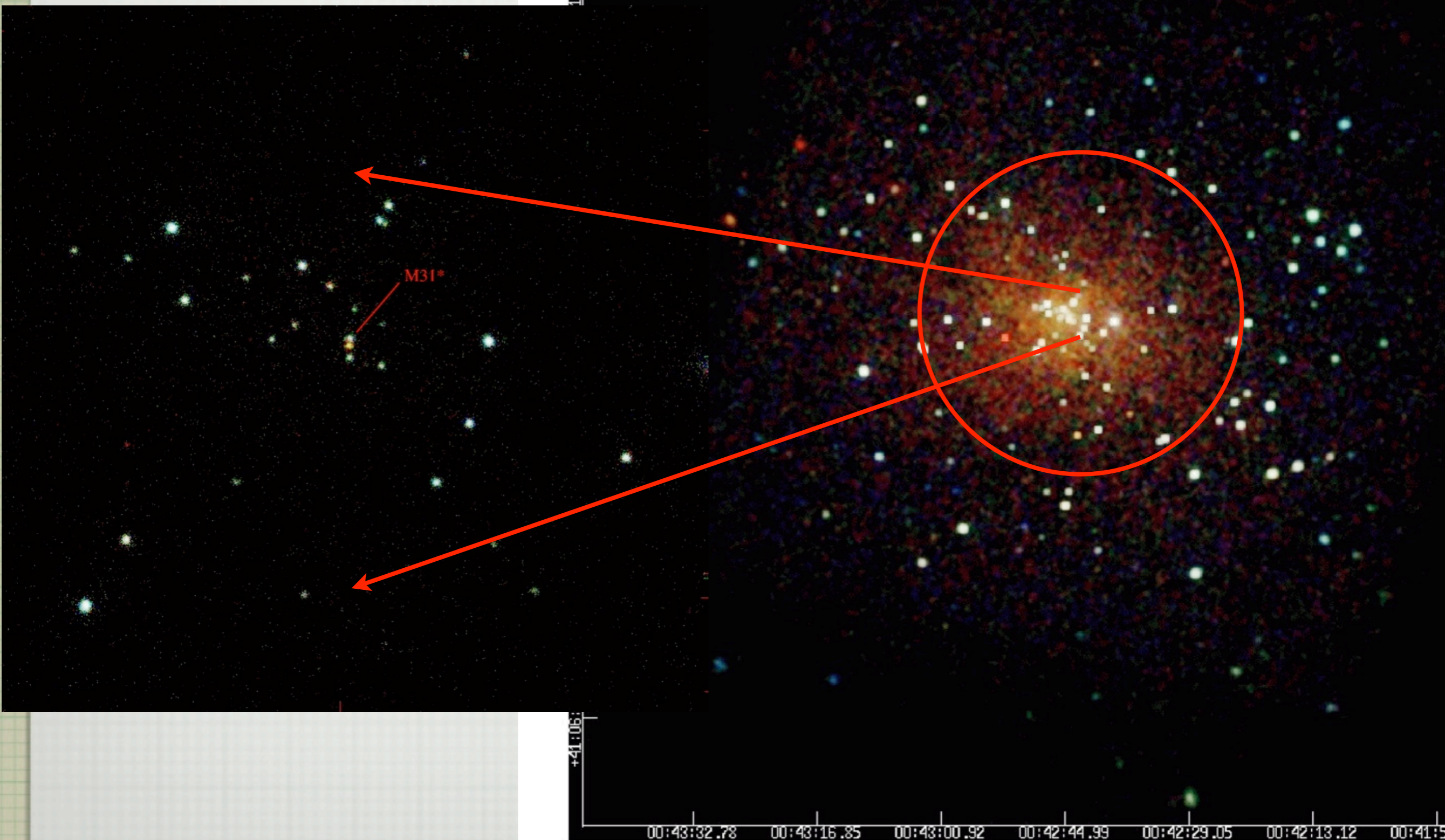
E

M31*

+41:06

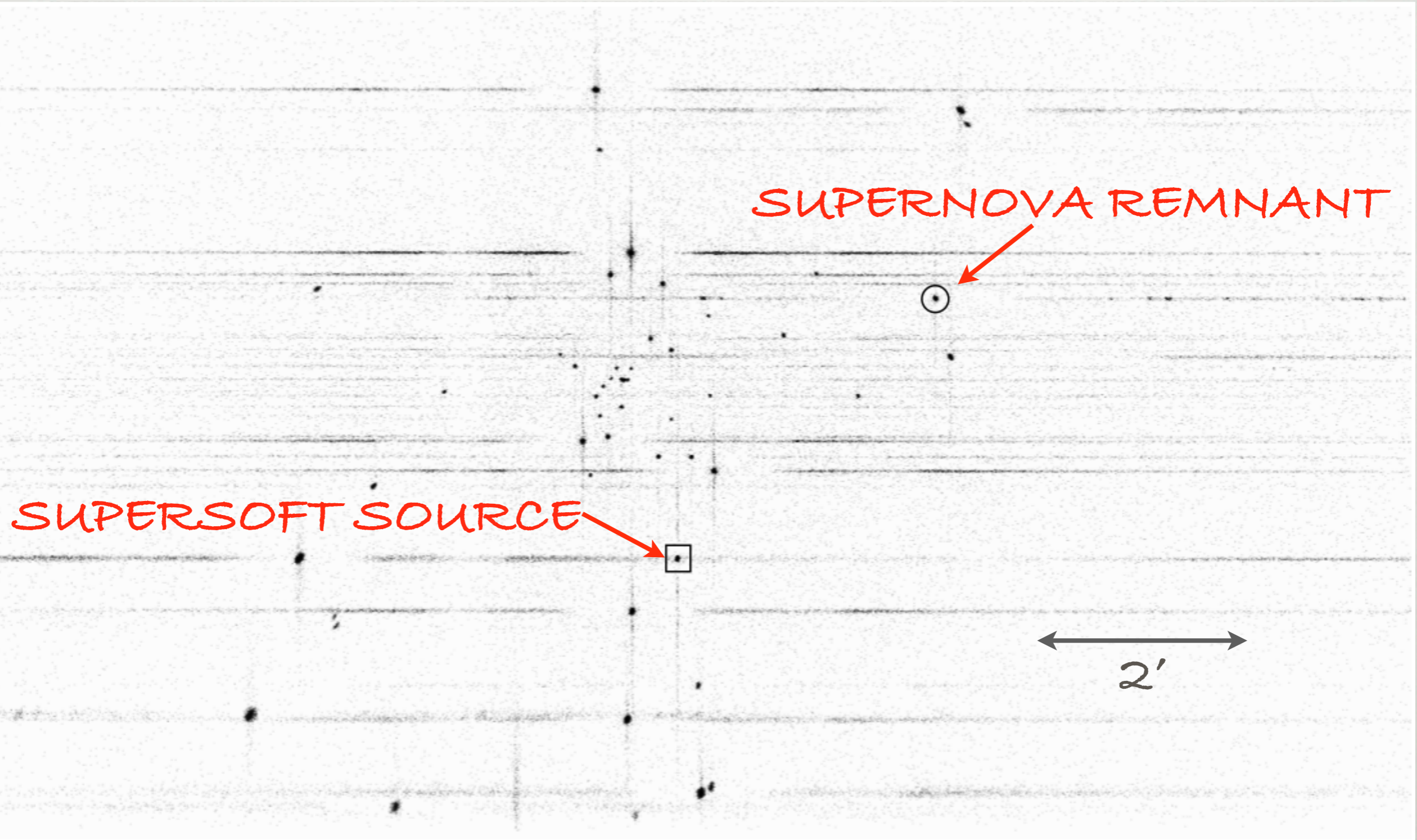
00:43:32.78 00:43:16.85 00:43:00.92 00:42:44.99 00:42:29.05 00:42:13.12 00:41:57

R.A. (J2000)



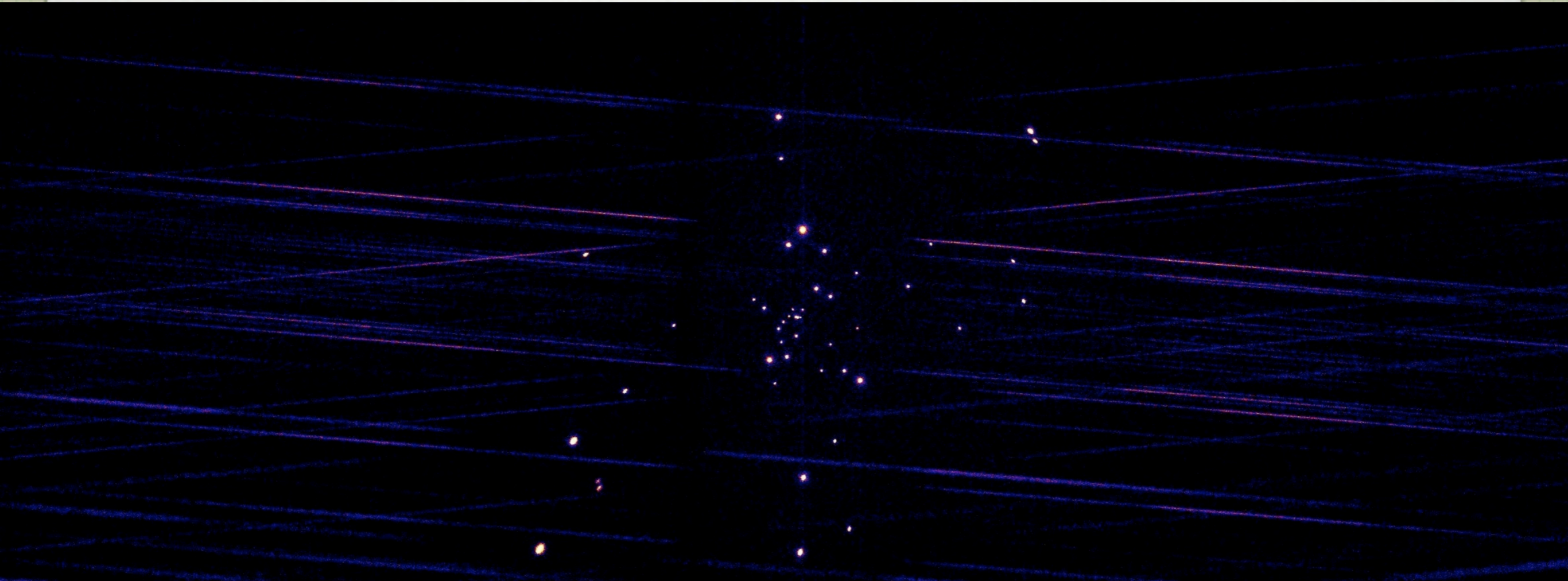
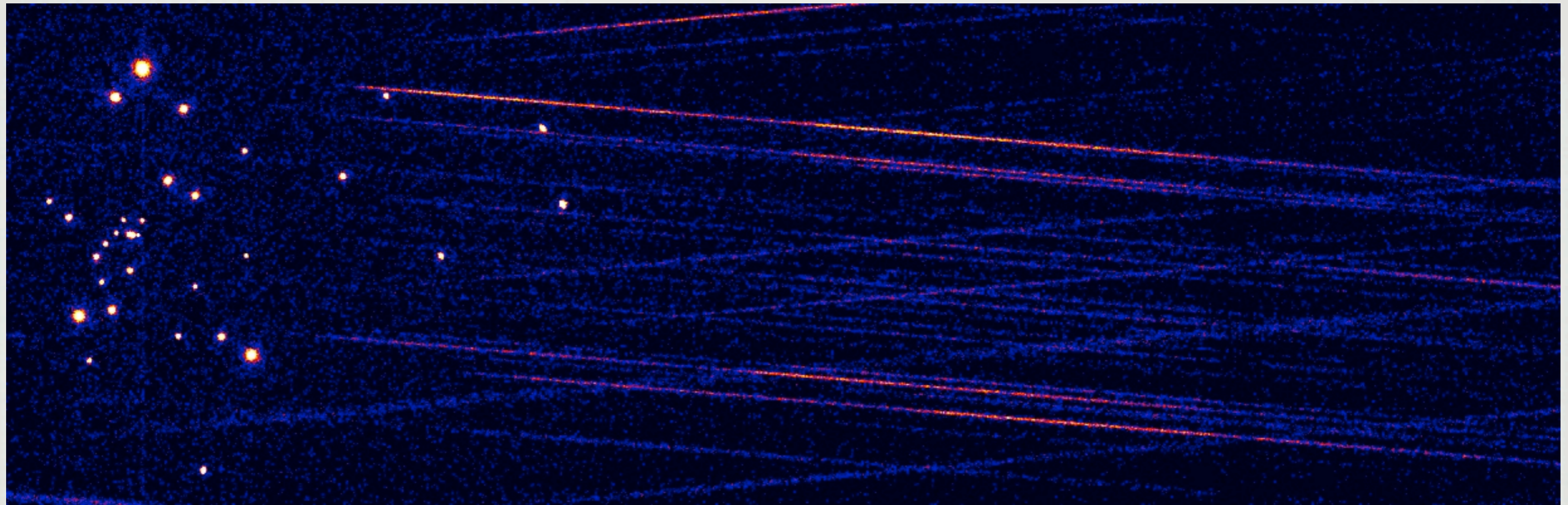
LETG/ACIS SIMULATION

250 KS



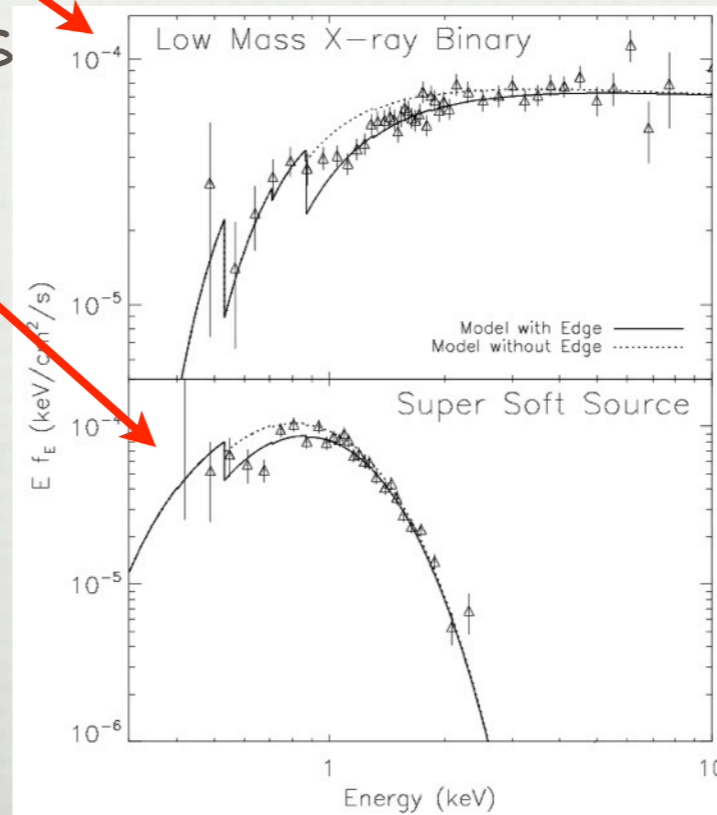
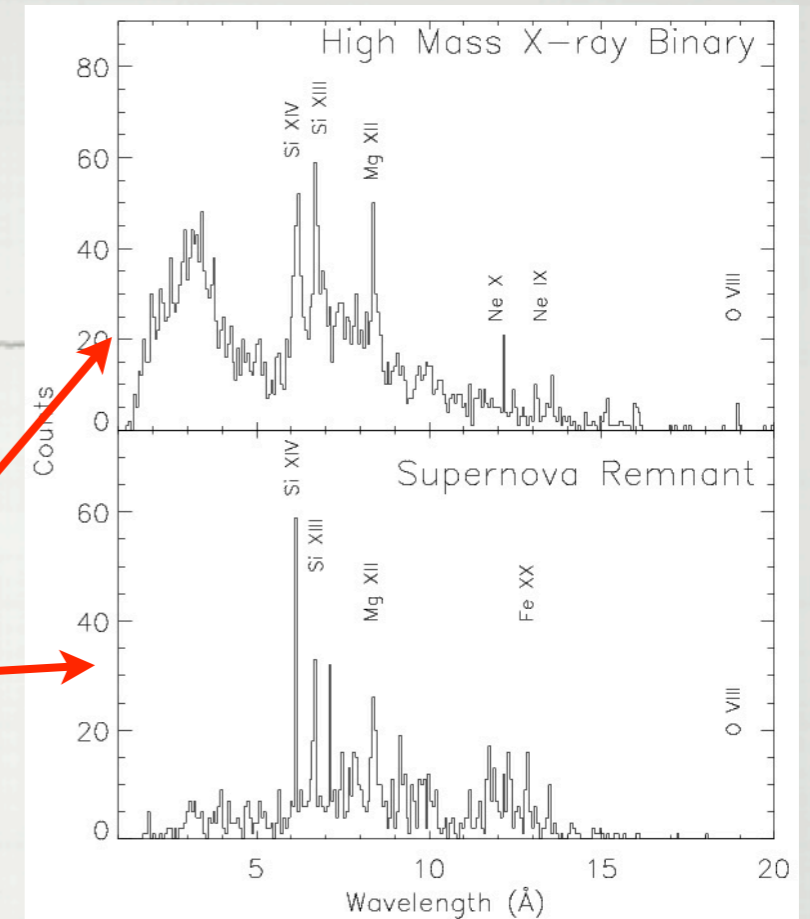
HETGS SIMULATION

750 KS



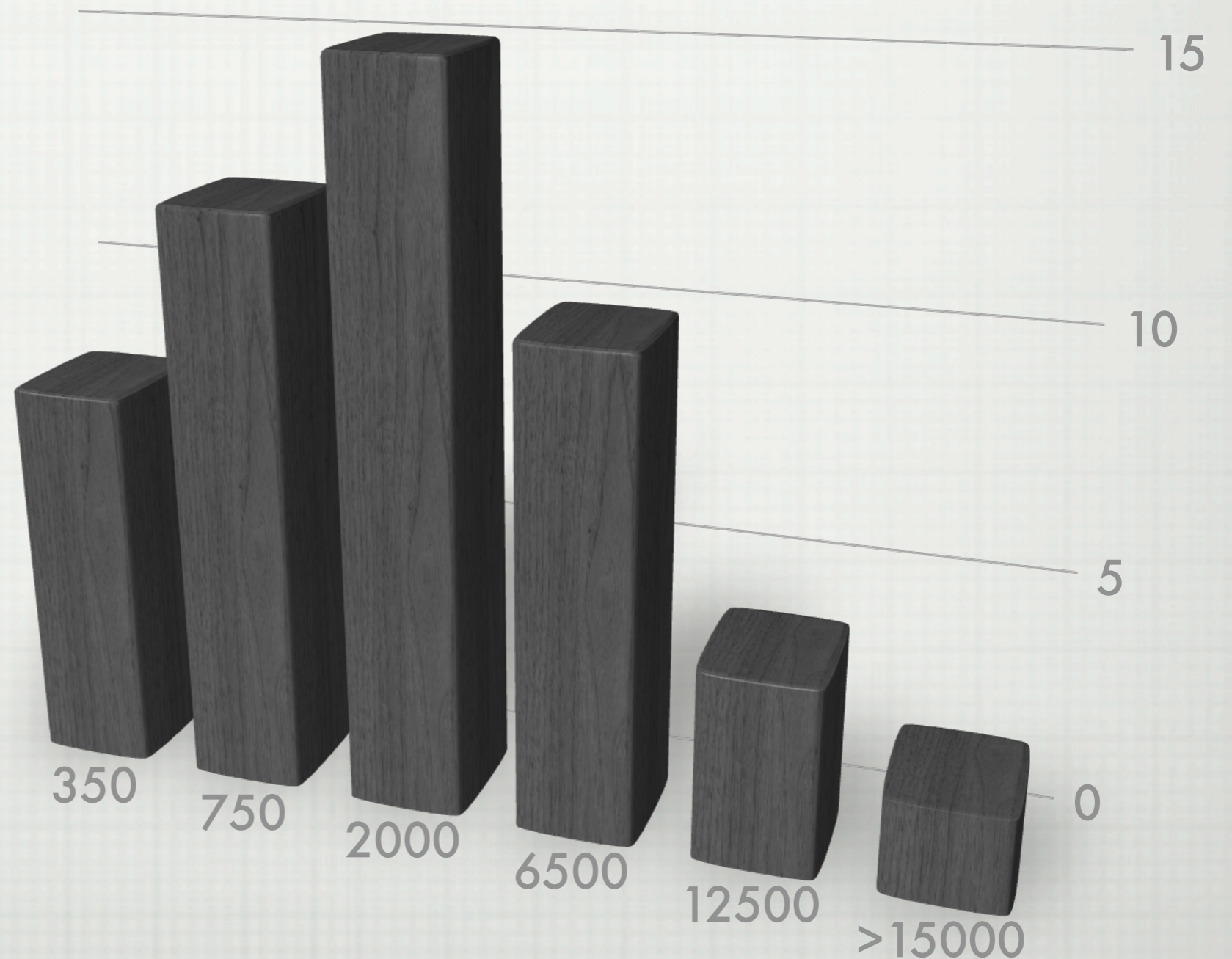
SCIENCE GOALS

- EMISSION LINES FROM HMXRB WINDS
- EMISSION LINES IN SNR
- ISM EDGES IN LMXRB
- ABUNDANCES IN LMXRBS
- SUPERSOFT SOURCES
- 1000 X-RAY BURSTS
- ODDITIES: SS 433, CIR X-1



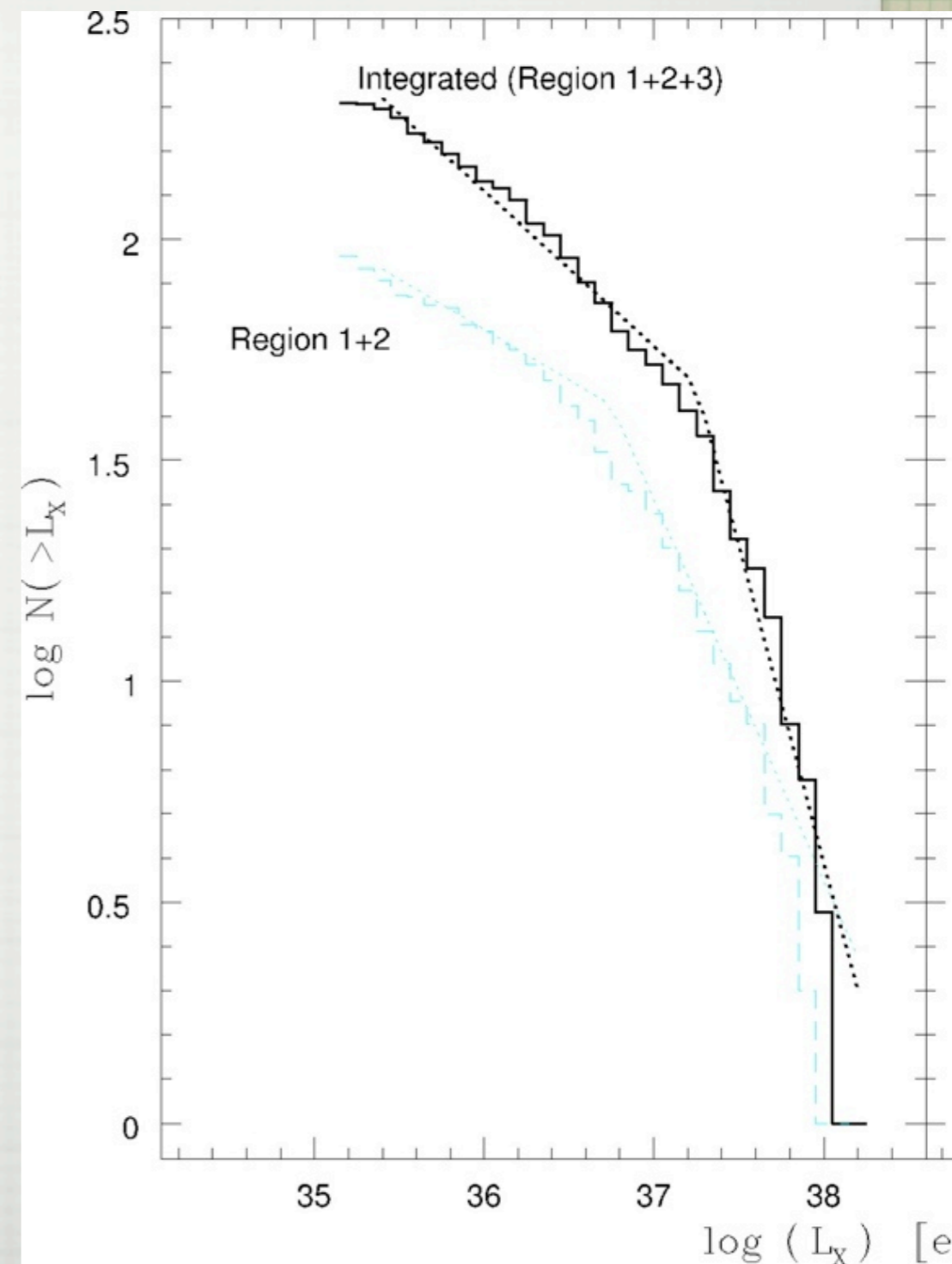
EXPECTED HETGS COUNTS

Count range	Number
>15000	2
10000-15000	4
3000-10000	10
1000-3000	15
500-1000	12
200-500	8



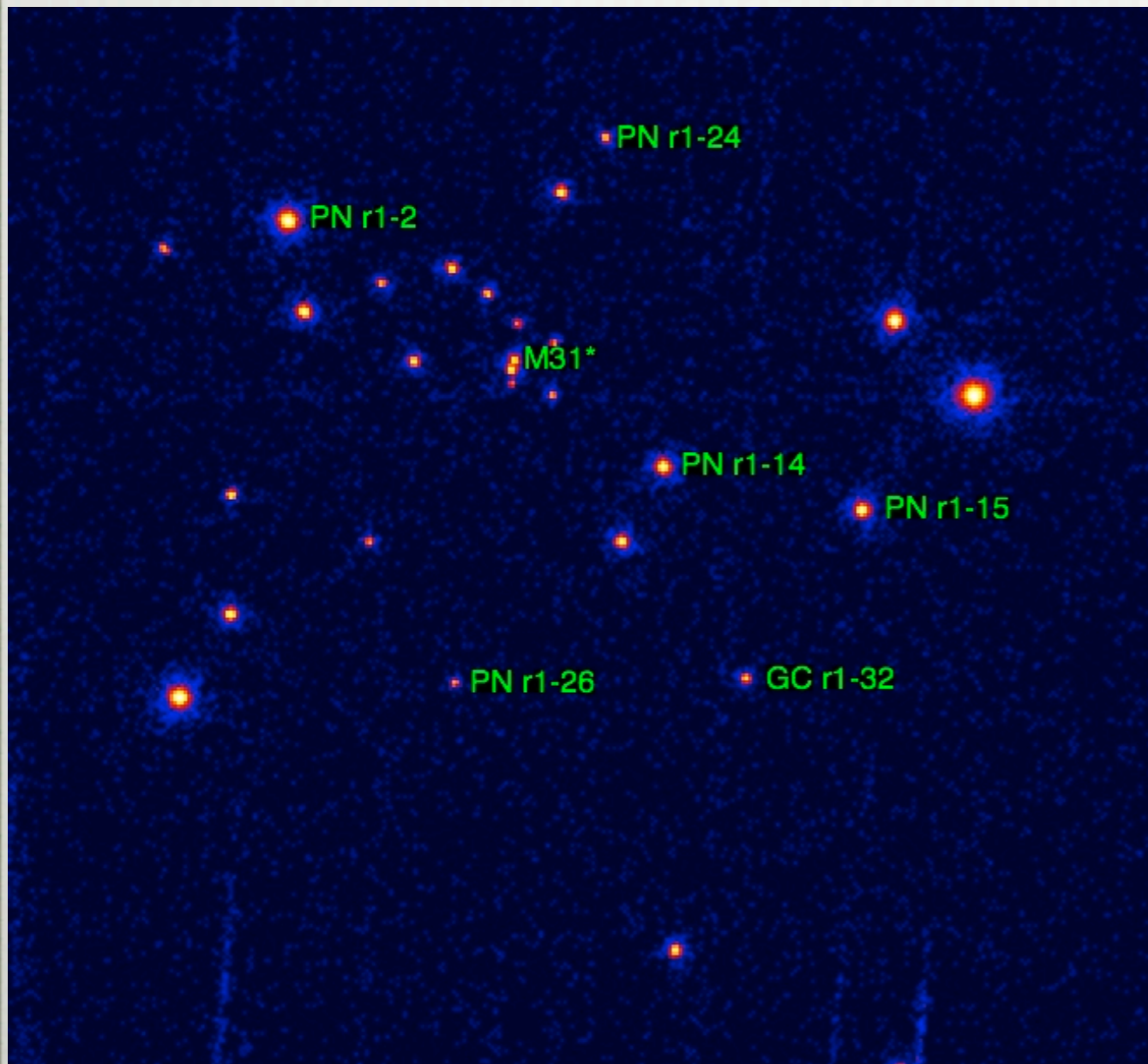
LUMINOSITY FUNCTIONS

- INNER BULGE (REGION 1): 2' X 2'
- FULL BULGE (REGION 2): 8' X 8'
- BULGE LF BREAK: 5×10^{36} ERG/S
- HETQS: 2000 COUNTS PER 10^{37} ERG/S
- BRIGHTEST SNR AT 6×10^{36} ERG/S
- >20,000 COUNT FOR NS WITH $L = L_{\text{EDD}}$



OPTICALLY IDENTIFIED PNE

□ SEVERAL BRIGHT PNE DETECTED IN BULGE, ANALOGS TO GX 3+1?



OPTICAL IDs				
ID	Chandra Name (CXOM31)	Type	Identification ^a	Radial Offset (arcsec)
r3-59	J004209.4+411745	GC	mita140	1.0
r3-54	J004212.1+411758	GC	Bo78, mita153	2.1, 0.9
r3-44	J004218.6+411401	GC	Bo86, mita164	1.1, 0.7
r3-74	J004219.6+412154	GC	mita165, 166	0.8, 0.7
r2-36	J004226.0+411915	GC	Bo96, mita174	1.6, 1.2
r2-33	J004231.2+411939	GC	Bo107, mita192	0.8, 0.9
r2-42	J004236.5+411350	Star	Ha94(238126)	0.1
r1-15	J004239.9+411547	PN ★	Ford17	2.9
r3-34	J004240.6+411032	GC	Bo123, mita212	2.9, 0.8
r3-33	J004240.9+412216	Star	Ha94(278717)	0.6
r1-32	J004241.4+411523	GC ★	mita213	1.5
r1-14	J004242.4+411553	PN ★	Ford4	2.9
r1-24	J004243.1+411640	PN ★	Ford322	0.6
r2-19	J004243.3+411319	Star	Ha94(235849)	0.5
r1-21	J004244.3+411605	PN ★	Ford316	2.9
r1-33	J004244.0+411604	1.6
r1-26	J004245.0+411523	PN ★	Ford21	0.8
r2-15	J004246.0+411736	GC	PB-in7	0.7
r1-2	J004247.1+411628	PN ★	Ford13	1.0
r2-56	J004250.4+411556	PN	Ford462	0.5
r3-71	J004250.7+411033	GC	mita222, PB-in2	0.5, 1.2
r3-69	J004253.6+412553	SNR	DO80(13)	6.0
r2-9	J004255.6+411835	GC	Bo138	2.5
r2-6	J004259.6+411919	GC	Bo143	1.7
r2-5	J004259.8+411606	GC	Bo144	2.2
r2-46	J004301.8+411726	Star	Ha94(261262)	0.6
r2-4	J004302.9+411522	GC	Bo146	1.9
r3-21	J004303.0+412042	PN	Ford201	2.4
r3-19	J004303.3+412122	GC	Bo147, mita240	2.5, 1.3
r2-2	J004303.8+411805	GC	Bo148	2.5
r3-83	J004306.6+412243	EO	MLA93(686)	0.9
r3-18	J004307.5+412020	GC	Bo150, mita246	2.8, 1.1
r3-15	J004310.6+411451	GC	Bo153, mita251	1.9, 0.4
r3-112	J004314.3+410725	GC	Bo158	2.3
r3-105	J004314.5+412513	GC	Bo159, mita258	1.4, 0.9
r3-10	J004315.4+411125	GC	mita260	0.9
r3-7	J004321.1+411751	PN	Ford209	1.7
r3-63	J004327.8+411829	SNR	DO80(15)	5.1
r3-1	J004337.2+411443	GC	mita299	0.6

^a Identifications as follows: mita = Magnier 1993; Bo = Battistini et al. 1987; Ha94 = Haiman et al. 1994; Ford = Ford & Jacoby 1978, Ciardullo et al. 1989; PB = Barmby 2001; DO80 = d'Odorico et al. 1980; MLA = SIMBAD.